Cancer Biol Med 2026. doi: 10.20892/j.issn.2095-3941.2026.0149

LETTER

Ferumoxytol triggers cancer ferroptosis *via* an NF-κB-driven IRONKILL mechanism

Tao Luo[1], Meng Li[1], Shijie Zhang[1], Kang Ding[1], Feng Gu[2], Qinguo Huang[3]

[1]Nanjing Hospital of Chinese Medicine, Nanjing University of Chinese Medicine, Nanjing 210000, China; [2]Department of Laboratory Medicine, Xuzhou Central Hospital, Southeast University, Xuzhou 221000, China; [3]Department of Neurosurgery, The Second Affiliated Hospital, Shantou University Medical College, Shantou 515000, China

Traditional radiotherapy and chemotherapy, despite killing tumor cells, often lack selectivity and therefore cause substantial collateral damage in patients[1]. Moreover, the ability of some cancer cells to evade these treatments may lead to relapse and metastasis[2]. Since 2012, ferroptosis has been a revolutionary approach in cancer therapy. Ferroptosis is driven by an abnormal accumulation of intracellular iron ions, which catalyze the buildup of lipid peroxides and ultimately disrupt cellular integrity[3]. This mechanism challenges conventional paradigms and offers a new strategy to combat refractory tumors that are resistant to apoptosis and prone to drug resistance. Because ferroptosis is triggered by iron-dependent lipid peroxidation (lipROS), a key question is how to selectively increase iron levels in tumor cells[4].

IRONKILL technology integrates ferumoxytol and DGDFi

Ferumoxytol (FMT) is an FDA-approved intravenous iron supplement for treating iron deficiency anemia in patients with chronic kidney disease. FMT selectively kills acute myeloid leukemia (AML) cells with low ferroportin (FPN) expression through iron overload and the Fenton reaction[5]. In AML cells, FMT accumulates primarily in lysosomes, whereas in normal cells, such as hematopoietic stem cells, it localizes in the cytoplasm, where it exhibits catalase-like activity and clears reactive oxygen species, thus indicating its safety for cancer therapy[6]. To extend the therapeutic potential of FMT to pan-cancer applications and enhance its anticancer efficacy, we developed a cancer cell-specific gene interference platform, DMP-miR (**Figures 1A and S1**). This platform consists of 3 components: an NF-κB decoy, a promoter, and a microRNA targeting the coding sequence of the gene of interest (**Figure 1B**). Cancer cells typically exhibit high NF-κB (p-p65) activity, which helps sustain malignancy, whereas normal cells show minimal activation[7]. We validated this finding by testing cancer cell lines (4T1, MC38, LLC, CT26, H22, Hepa1-6, GL261, B16F10, C1498, Pan02, BGC823, MDA-MB-453, and A549) and normal cell lines (MPC-5, MLE-15, McCoy, NIH-3T3, L929, HT22, NMuMG, AML-12, HL-1, C2C12, GES-1, MCF12A, and MRC5) (**Figures 1C and S2A**). Therefore, DMP-miR enables specific gene interference in cancer cells.

Herein, we combined knockdown of the lysosomal enzyme GBA (glucocerebrosidase) and the iron efflux transporter FPN to construct the gene interference vector DGDFi (DMP-miGBA-DMP-miFPN) (**Figures 1A, B and S1, Tables S1–S3**). Although lysosomes are known to serve as intracellular iron pools, the role of GBA in iron metabolism remains unclear. GBA hydrolyzes glucosylceramide (GlcCer) to ceramide (Cer) and glucose (Glu), and is a key enzyme maintaining lysosomal lipid metabolism and membrane composition homeostasis[8]. We hypothesized that GBA inactivation would induce lysosomal storage disorders and damage, thus leading to the release of free iron and triggering lipROS *via* the Fenton reaction. Additionally, FPN knockdown inhibits iron efflux, thereby causing iron accumulation and promoting ferroptosis in cancer cells. Importantly, FMT, by acting as an iron supplement, exacerbates DGDFi-induced ferroptosis and leads to potent death of pan-cancer cells. We termed this strategy IRONKILL.

To ensure *in vivo* safety, we administered IRONKILL at an FMT concentration of 50 μg/mL, which showed low toxicity in both cancer and normal cells (**Figure S3**). For subsequent experiments, we selected cancer and normal cell pairs, including 4T1, LLC, and Hepa1-6, and their normal counterparts, NMuMG, MLE-15, and AML-12. Evaluation of the gene interference efficiency of IRONKILL indicated significant

Correspondence to: Tao Luo, Feng Gu and Qinguo Huang
E-mail: luotao@hnu.edu.cn, gufeng2679@126.com and hqghcjr0920@126.com
ORCID ID: https://orcid.org/0000-0001-8675-6762, https://orcid.org/0000-0002-9874-6307 and https://orcid.org/0009-0005-3262-7179
Received March 13, 2026; accepted April 20, 2026;
published online May 20, 2026.
Available at www.cancerbiomed.org
©2026 The Authors. Creative Commons Attribution-NonCommercial 4.0 International License (CC BY-NC 4.0)

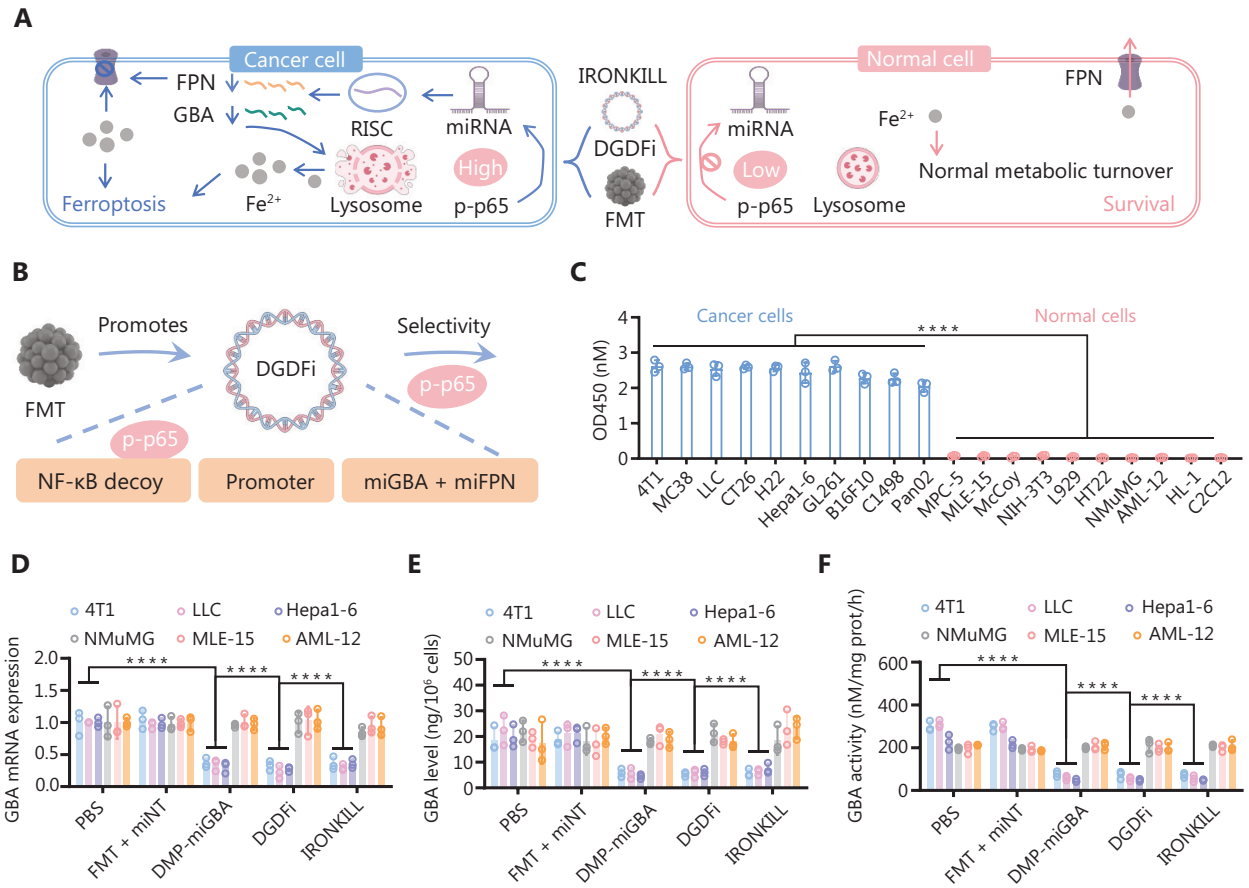


Figure 1 Continued

decreases in *GBA* mRNA and protein levels, and consequently GBA activity in cancer cells; moreover, FMT did not interfere with DMP-miGBA or DGDFi-mediated gene knockdown (**Figure 1D–F**). *GBA* inhibition resulted in excessive accumulation of the GlcCer substrate in lysosomes, thereby inducing lysosomal damage (increased Galectin-3-positive cells, decreasing LysoTracker fluorescence, and elevating *Lamp1*/*Lamp2* expression); these findings together suggested compromised lysosomal iron storage (**Figures 1G, H and S4, S5**). Subsequently, measurement of intracellular Fe^{2+} levels revealed that *GBA* knockdown triggered substantial Fe^{2+} release in cancer cells (**Figure 1I**). Notably, lysosomal damage was prevented in normal cells, because *GBA* remained unaffected, given the cells' low p-p65 levels (**Figures 1C–I and S2, S4 and S5**). Additionally, DMP-FPN or DGDFi-mediated *FPN* knockdown significantly suppressed *FPN* mRNA and protein expression, and further increased intracellular Fe^{2+} levels, in cancer cells, whereas normal cells remained unaffected (**Figure 1J–L**). Importantly, FMT supplementation did not interfere with IRONKILL-mediated *FPN* knockdown and further elevated Fe^{2+} levels in cancer cells (**Figure 1J–L**). These findings demonstrated that IRONKILL selectively modulated iron metabolism in cancer cells and led to a substantial increase in Fe^{2+} content.

IRONKILL triggers marked ferroptosis in pan-cancers

Given the substantial elevation in Fe^{2+} levels, we assessed cell viability. IRONKILL effectively killed cancer cells without affecting normal cells (**Figure S6**). To confirm the mechanism of cancer cell death, we examined ferroptosis markers, including lipROS and GPX4 activity. IRONKILL significantly increased lipROS levels and GPX4 activity in cancer cells, thus indicating ferroptosis induction (**Figures 1M, N and S7**). Moreover, the absence of such effects in normal cells confirmed that IRONKILL is a cancer cell-specific ferroptosis inducer (**Figures 1M, N and S4, S8**). Compared with DGDFi alone, IRONKILL exhibited enhanced cancer cell killing and lipROS production, in synergy with FMT (**Figures 1M, N and S6–S8**). Furthermore, the significant reversal of IRONKILL-induced cell death by the ferroptosis inhibitor liproxstatin-1 (lip1) confirmed ferroptosis as

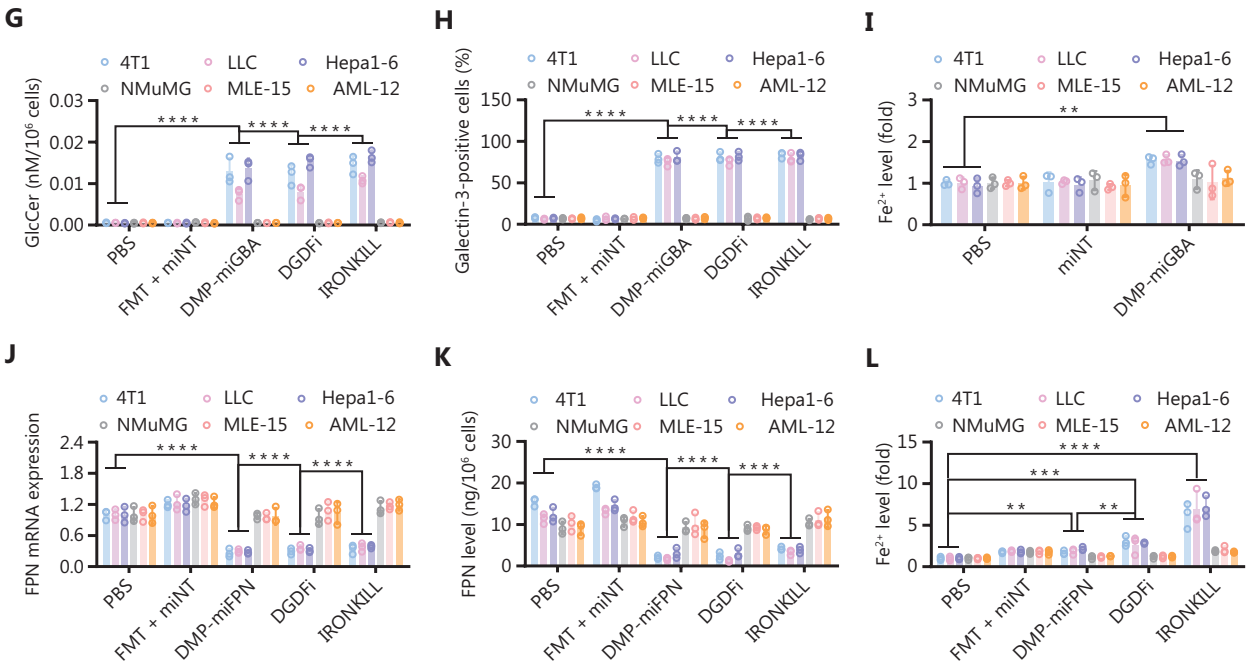


Figure 1 Continued

the mechanism (**Figure 1O**). Additionally, treatment with the NF-κB inhibitor BAY 11-7082 abrogated *FPN* and *GBA* knockdown, and consequently prevented cancer cell death; these findings further supported that IRONKILL functions in an NF-κB-dependent manner, thus ensuring *in vivo* safety (**Figure S9**).

To further validate the *in vivo* ferroptosis-inducing effect of IRONKILL, we engineered DGDFi into an adeno-associated virus (AAV2 serotype) and tested it in 5 tumor models (three solid tumors and 2 hematologic malignancies). AAV2 was selected for *in vivo* delivery because of its broad tropism, in alignment with the pan-cancer approach of this study. Because of its well-established safety profile (low immunogenicity and minimal genomic integration) and extensive prior validation, it provided reliable benchmarks for transduction and biodistribution. IRONKILL exhibited broad anti-tumor efficacy against various *in vivo* tumors (4T1 subcutaneous breast cancer model, LLC subcutaneous lung cancer model, Hepa1-6 liver cancer model, and WEHI-3 and C1498 intravenous acute myeloid leukemia models): 60% of mice survived tumor-free for more than 100 days **(Figures 1P–R and S10**). This prolonged survival also supported the *in vivo* safety of IRONKILL. Moreover, the reversal of IRONKILL's efficacy by lip1 further confirmed that its *in vivo* therapeutic mechanism was ferroptosis (**Figures 1P–R and S10**). We subsequently measured tumor iron content, which was generally higher in the IRONKILL-treated group than the other groups. Notably, the significant reversal of iron accumulation in the IRONKILL group after lip1 treatment further supported that the tumor-killing mechanism of IRONKILL was ferroptosis (**Figure S11**). Although AAV2 shows good efficacy in mice, clinical translation might require alternative systems (e.g., lipid nanoparticles), because of AAV immunogenicity in humans. This caveat does not diminish AAV2's utility for proof-of-concept studies but may inform future clinical development. In summary, IRONKILL integrated the iron-supplementing function of FMT with the disruption of lysosomal iron pools and cellular iron efflux mechanisms, and markedly elevated intracellular Fe^{2+} levels in cancer cells. This technology demonstrated potent ferroptosis-inducing activity against pan-cancers and has substantial promise for clinical application.

Innovation and challenges of IRONKILL

The innovation of IRONKILL lies in its strategic approach: rather than suppressing the high NF-κB activity in cancer cells, it exploits this feature as a precise entry point for attack. However, systemic inflammatory states might transiently elevate NF-κB in normal tissues; this challenge could be addressed through careful patient selection, monitoring of inflammatory markers such as C-reactive protein, and, if needed, anti-inflammatory pre-treatment. In a similar paradigm, rigorous management in the arsenic trioxide treatment of acute promyelocytic leukemia has transformed a potent toxin into a life-saving therapy[9,10]. Both approaches demonstrate that in highly lethal malignancies, therapeutic success

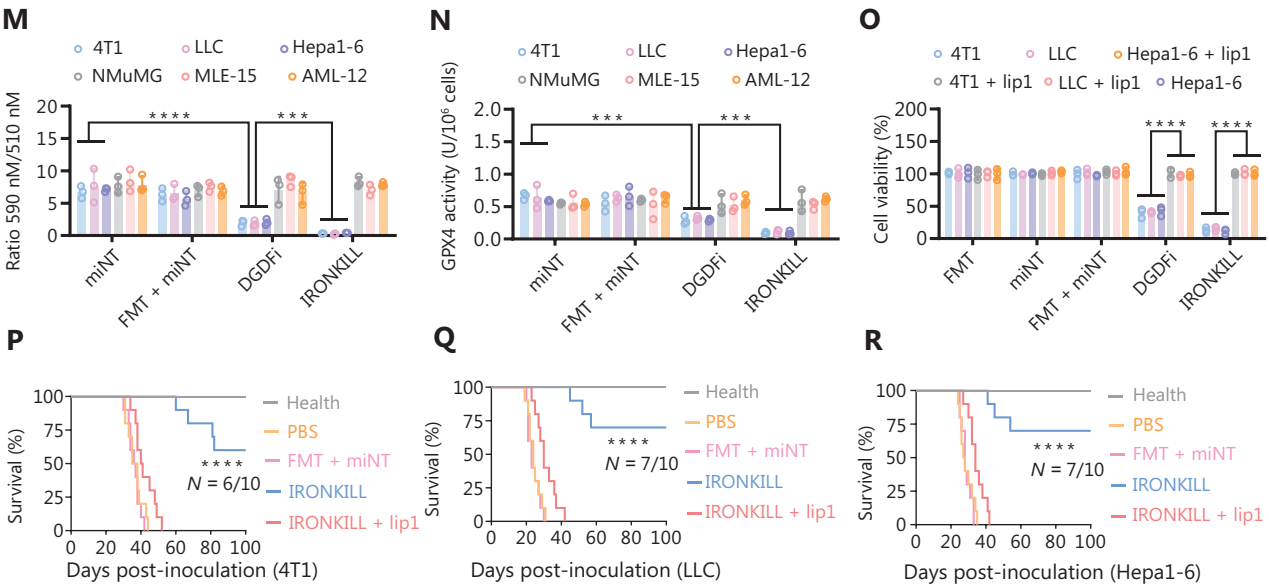


Figure 1 FMT enhances ferroptosis interfered by GBA and FPN in cancer gene therapy. (A) Schematic model of the IRONKILL technology mechanism. IRONKILL selectively responds to the high expression of p-p65 in cancer cells and expresses microRNAs that knock down *GBA* and *FPN*, thus significantly increasing Fe^{2+} levels within the cancer cells. Meanwhile, FMT further induces intracellular iron accumulation and results in pronounced ferroptosis in tumors. Normal cells, because of their low expression of p-p65, escape the cytotoxic effects of IRONKILL. (B) Introduction to IRONKILL technology, encompassing FMT, an NF-κB-based DMP vector, miGBA, and miFPN. (C) p-p65 expression level. (D) *GBA* mRNA expression level. (E) GBA protein level. (F) GBA activity assay. (G) Quantification of the GBA substrate GlcCer. (H) Statistical data for galectin-3-positive cells. (I) Cellular Fe^{2+} content after treatment with PBS, miNT, or DMP-miGBA. (J) *FPN* mRNA expression level. (K) FPN protein level. (L) Cellular Fe^{2+} content after treatment with PBS, FMT + miNT, DMP-miFPN, DGDFi, or IRONKILL. (M) Cellular lipROS measurement, presented as the ratio of reduced state fluorescence intensity at 590 nm to oxidized state fluorescence intensity at 510 nm. (N) GPX4 activity assay. (O) Cell viability after treatment with FMT, miNT, FMT + miNT, DGDFi, or IRONKILL. Cells were harvested for data collection after overnight plasmid transfection, and FMT (50 μg/mL) was added as indicated and incubated for 48 h. Kaplan–Meier survival curves for (P) 4T1 breast cancer mice (s.c., n = 10), (Q) LLC lung cancer mice (s.c., n = 10), and (R) Hepa1-6 liver cancer mice (s.c., n = 10). For *in vivo* IRONKILL administration, FMT and DGDFi were administered at doses of 2 mg/kg and 10^{11} vg/mouse, respectively, as a single combined dose. Lip1 (10 mg/kg, i.p.) was used to perform the ferroptosis rescue assays. *GBA*, glucocerebrosidase gene; *FPN*, ferroportin gene; MT, ferumoxytol; DGDFi, DMP-miGBA-DMP-miFPN; LipROS, lipid peroxidation; s.c., subcutaneous injection; Lip1, liproxstatin-1; i.p., intraperitoneal injection. Statistical analysis and graphing were performed in GraphPad Prism 8.0.

hinges not on avoiding risk but on controlling it through mechanistic insight and clinical vigilance. IRONKILL thus offers a critical evolution in oncology, by embracing biological complexity to achieve safer, more effective outcomes. This novel pan-cancer therapeutic strategy is ultimately aimed at providing a safe, clinically translatable approach that achieves potent efficacy across multiple tumor models and enables long-term tumor-free survival.

Grant support

This work was supported by the National Natural Science Foundation of China (Grant No. 82400186), the Natural Science Foundation of Jiangsu Province (Grant No. BK20240269), the Jiangsu Province Young Scientific and Technological Talents Promotion Program (Grant No. JSYJ-2025-728), the Feihong Program of Nanjing Hospital of Chinese Medicine (Grant No. FHJH202402), the Medical Scientific Research Foundation of Guang Dong Province (Grant No. A2023409), the Shantou Medical Health Science and Technology Plan (Grant No. 220518116490852), and the Guang Dong Basic and Applied Basic Research Foundation (Grant No. 2026A1515012831).

Conflict of interest statement

No potential conflicts of interest are disclosed.

Author contributions

Conceived and designed the analysis: Tao Luo, Meng Li, Qinguo Huang.
Collected the data: Shijie Zhang, Qinguo Huang.
Contributed data or analysis tools: Kang Ding, Feng Gu.

Performed the analysis: Feng Gu, Qinguo Huang.
Wrote the article: Tao Luo, Feng Gu, Qinguo Huang.

Data availability statement

The data generated in this study are available upon request from the corresponding author.

Ethics statement

All animal experiments were performed in accordance with protocols sanctioned by the Animal Ethical and Welfare Committee (AEWC) at the Shenzhen Glorybay Biomedical Laboratory Animal Center (approval No. RW-IACUC-24-0132).

References

1. Yazbeck V, Alesi E, Myers J, Hackney MH, Cuttino L, Gewirtz DA. An overview of chemotoxicity and radiation toxicity in cancer therapy. Adv Cancer Res. 2022; 155: 1-27.
2. Zafar A, Khatoon S, Khan MJ, Abu J, Naeem A. Advancements and limitations in traditional anti-cancer therapies: a comprehensive review of surgery, chemotherapy, radiation therapy, and hormonal therapy. Discov Oncol. 2025; 16: 607.
3. Dixon SJ, Olzmann JA. The cell biology of ferroptosis. Nat Rev Mol Cell Biol. 2024; 25: 424-42.
4. Wahida A, Conrad M. Decoding ferroptosis for cancer therapy. Nat Rev Cancer. 2025; 25: 910-24.
5. Trujillo-Alonso V, Pratt EC, Zong H, Lara-Martinez A, Kaittanis C, Rabie MO, et al. FDA-approved ferumoxytol displays anti-leukaemia efficacy against cells with low ferroportin levels. Nat Nanotechnol. 2019; 14: 616-22.
6. Wang Q, Qian W, Han Y, Mao Y, Gao Z, Chen Y, et al. Ferumoxytol promotes haematopoietic stem cell post-injury regeneration as a reactive oxygen species scavenger. Nat Nanotechnol. 2025; 20: 959-69.
7. Ebrahimi N, Abdulwahid ARR, Mansouri A, Karimi N, Bostani RJ, Beiranvand S, et al. Targeting the NF-κB pathway as a potential regulator of immune checkpoints in cancer immunotherapy. Cell Mol Life Sci. 2024; 81: 106.
8. Milenkovic I, Blumenreich S, Futerman AH. GBA mutations, glucosylceramide and Parkinson's disease. Curr Opin Neurobiol. 2022; 72: 148-54.
9. Yan M, Wang H, Wei R, Li W. Arsenic trioxide: applications, mechanisms of action, toxicity and rescue strategies to date. Arch Pharm Res. 2024; 47: 249-71.
10. Jiang Y, Shen X, Zhi F, Wen Z, Gao Y, Xu J, et al. An overview of arsenic trioxide-involved combined treatment algorithms for leukemia: basic concepts and clinical implications. Cell Death Discov. 2023; 9: 266.

Cite this article as: Luo T, Li M, Zhang S, Ding K, Gu F, Huang Q. Ferumoxytol triggers cancer ferroptosis *via* an NF-κB-driven IRONKILL mechanism. Cancer Biol Med. 2026; 23: 1341-1345. doi: 10.20892/j.issn.2095-3941.2026.0149